

Orbital and maxillofacial computer aided surgery: patient-specific finite element models to predict surgical outcomes

VINCENT LUBOZ^{†*}, MATTHIEU CHABANAS[†], PASCAL SWIDER[‡] and YOHAN PAYAN^{†*}

[†]TIMC Laboratory, UMR CNRS 5525, University J. Fourier, 38706 La Tronche, France

[‡]Biomechanics Laboratory, IFR 30, Purpan University Hospital, 31059 Toulouse cedex 3, France

This paper addresses an important issue raised for the clinical relevance of Computer-Assisted Surgical applications, namely the methodology used to automatically build patient-specific finite element (FE) models of anatomical structures. From this perspective, a method is proposed, based on a technique called the mesh-matching method, followed by a process that corrects mesh irregularities. The mesh-matching algorithm generates patient-specific volume meshes from an existing generic model. The mesh regularization process is based on the Jacobian matrix transform related to the FE reference element and the current element.

This method for generating patient-specific FE models is first applied to computer-assisted maxillofacial surgery, and more precisely, to the FE elastic modelling of patient facial soft tissues. For each patient, the planned bone osteotomies (mandible, maxilla, chin) are used as boundary conditions to deform the FE face model, in order to predict the aesthetic outcome of the surgery. Seven FE patient-specific models were successfully generated by our method. For one patient, the prediction of the FE model is qualitatively compared with the patient's post-operative appearance, measured from a computer tomography scan. Then, our methodology is applied to computer-assisted orbital surgery. It is, therefore, evaluated for the generation of 11 patient-specific FE poroelastic models of the orbital soft tissues. These models are used to predict the consequences of the surgical decompression of the orbit. More precisely, an average law is extrapolated from the simulations carried out for each patient model. This law links the size of the osteotomy (i.e. the surgical gesture) and the backward displacement of the eyeball (the consequence of the surgical gesture).

Keywords: Computer-assisted surgery; Orthognathic surgery; Exophthalmia; Finite element modelling; Patient-specific meshing; Mesh regularization

1. Introduction

Computer aided surgery (CAS) is a growing research domain, with systems aiming at assisting surgeons for the realization of diagnostic and therapeutic gestures in a rational and quantitative way while trying to increase safety and accuracy (Taylor *et al.* 1996). The first designed systems focused on orthopaedics, such as the computer-aided technique proposed by Lavallée *et al.* (1995) and Merloz *et al.* (1997) for accurate transpedicular screw fixation during spine surgery. The idea consisted of (1) building a 3D geometrical model of the pedicle from a computer tomography (CT) exam of the patient, (2) planning the optimal screw position in the 3D model, and (3) per-operatively guiding the surgeon by tracking the screw orientation with a 3D optical localizer. More

recently, researchers addressed CAS protocols dedicated to anatomical structures that cannot be considered as “rigid” as they are mainly composed of biological soft tissues, like brain (Skrinjar *et al.* 2002), liver (Blackall *et al.* 2001), face (Chabanas *et al.* 2003), breast (Azar *et al.* 2002), or orbit (Luboz *et al.* 2004). The corresponding CAS systems therefore, need to take into account the displacements of the anatomical structures as well as their deformations. In most cases, authors propose to build biomechanical models of the anatomical structures and use these models to predict the tissue deformations induced by the surgical gesture (as a consequence, for example, of a modification of the boundary conditions, or because of the insertion of a biopsy needle). Most authors face two main problems with the compatibility/acceptability of their CAS systems with the clinical routine

*Corresponding authors. E-mail: yohan.payan@imag.fr; vincent.luboz@imag.fr

framework: (1) the soft tissues biomechanical models should be “interactive”; in other words, a model needing one or two hours to give numerical results will be less acceptable to surgeons; (2) the pre-operative building of each new patient model (with a new morphology) should, here again, be fast enough to be used by surgeons.

Some solutions have been proposed to face the first issue; in particular, the introduction of continuous modeling approaches whose computation times allow “interactive” manipulation of the 3D model (see Picinbono *et al.* (2003), for example).

This paper aims at introducing and illustrating the method proposed by our group to address the second issue. This method, originally published under the name of mesh-matching procedure (Couteau *et al.* 2000), is used here to introduce an algorithm that aims at correcting irregularities of 3D model meshes in order to perform finite element (FE) computations. The first part of the paper describes the principles underlying the complete method to allow an automatic generation of a 3D FE mesh adapted to each patient’s morphology. Then, this methodology is illustrated with two clinical CAS applications, namely orthognathic and orbital surgeries.

2. Generation of patient-specific finite element models

2.1 Principles

Five steps define the method for generating patient-specific finite element models:

1. An FE model of the anatomical structure is chosen as a starting point. This model is often built from a standard patient morphology. Its 3D mesh is assumed to be optimal in terms of mesh refinement and mesh regularity. This model is called the “generic model” since it is used to define other FE meshes of the same anatomical structure corresponding to other patient morphologies.
2. The external surface of the patient anatomical structure is extracted from CT (or MRI) data. On each CT (or MRI) slice, the external contour of the structure is segmented, providing a set of 3D points located on the surface.
3. An elastic registration method, originally proposed in the field of computer-assisted surgery (Lavallée 1996; Szeliski and Lavallée 1996), is used to match the extracted patient surface points with the nodes located on the external surface of the generic FE model, through a volumetric transform \mathbf{T} . This function \mathbf{T} is a combination of a global *rigid* transform, which aligns the two datasets, and local *elastic* transforms, which consist in cubic B-Splines functions defined on an adaptative octree that encloses the data. The parameters of \mathbf{T} are obtained through an optimization process that minimizes the Euclidian distance between the two surfaces, namely the points extracted from the patient data and the external nodes of the generic FE model.
4. The volumetric transform \mathbf{T} is then applied to every node of the FE generic mesh, namely the nodes located on the external surface as well as the internal nodes that define the FE volume. A new volumetric mesh is thus automatically obtained by assembling the transformed nodes into elements, with a topology similar to that of the generic FE model with the same number of elements and the same element types.
5. The regularity of the patient 3D mesh is checked in order to see if FE analysis can be performed. If some elements of the mesh are detected as irregular, a global mesh regularization technique is proposed.

Steps 1–4 were originally published under the name of the mesh-matching algorithm (Couteau *et al.* 2000). This method was introduced to automatically generate customized hexahedron and wedge 3D patient meshes from an existing 3D generic mesh. The algorithm was successfully applied to proximal (Couteau *et al.* 2000) and entire (Luboz *et al.* 2001) femora. However, the application to a more complicated geometry, namely a FE model of the human face (Chabanas and Payan 2000), provided mesh irregularities that made the mechanical analysis impossible. For this reason, the fifth step was added to the global algorithm, in order to correct irregularities from the generated patients’ meshes. The next part describes this regularization algorithm.

2.2 Regularization of the mesh

2.2.1 Regularity criteria. The objective of the regularization algorithm is not to improve the quality of the FE mesh, but to correct the mesh irregularities that preclude the FE analysis. By regularity, we mean a criterion that is associated with the Jacobian matrix transform, coupling the reference element (unit reference framework) and the actual element (real reference framework) (Touzot and Daht 1984; Zienkiewicz and Taylor 1994). FE analysis is carried out only if the transform can be computed on each point inside the element, that is to say if the Jacobian determinant value ($\det \mathbf{J}$) is positive anywhere inside the element. The Jacobian determinant $\det \mathbf{J}$ is then computed at each node of each element. If a negative or nil value is obtained for one of the nodes, the element is classified as irregular.

2.2.2 Regularization algorithm. The regularization algorithm consists of an iterative process: nodes of irregular elements are slightly shifted at each step, until each element becomes regular. In the following development, the subscript variables are: k - irregular element; i - node(s) of element k with nil or negative Jacobian determinant; j - nodes attached to element k ; n - number of nodes of element k .

The regularization procedure consists of two main steps:

- (1) Computation of the Jacobian determinant (which has no dimension) at each node of the mesh and detection of irregular element k ($\det \mathbf{J}_i \leq 0$).

- (2) Automatic correction of irregular element k using a numerical sensitivity procedure based on gradient evaluation.

The idea is to iteratively move each node i (where $\det \mathbf{J}_i \leq 0$) in a direction that tends to increase the $\det \mathbf{J}_i$ value. As an analytical expression of the gradient vector $\nabla(\det \mathbf{J}_i)_j$ can be found, the algorithm consists of moving the node in the direction of the gradient vector in order to increase $\det \mathbf{J}_i$.

As expressed in equation (1), the gradient vector $\nabla(\det \mathbf{J}_i)_j$ (whose dimension is: length^{-1}) is first computed using actual coordinates $\mathbf{X}_j(x_j, y_j, z_j)$ of nodes j attached to the distorted element k (with a first order Taylor Series). This gradient vector provides an evaluation of the sensitivity of the geometrical transform (reference framework / actual framework) to the nodes locations. Analytical expressions of $\det \mathbf{J}_i$ and $\nabla(\det \mathbf{J}_i)_j$ are derived using a computer algebra system (Maple©).

$$\nabla(\det \mathbf{J}_i)_j = \begin{bmatrix} \frac{\partial \det \mathbf{J}_i}{\partial x_j}(x_j) \\ \frac{\partial \det \mathbf{J}_i}{\partial y_j}(y_j) \\ \frac{\partial \det \mathbf{J}_i}{\partial z_j}(z_j) \end{bmatrix} \quad \text{where } j = 1 \dots n. \quad (1)$$

The directional vector \mathbf{V}_j , expressed by equation (2), is determined for updating the node locations. The dimension of \mathbf{V}_j is length. For a node with index j , the gradient vectors (1) are summed at the element k level. If n is the number of nodes of this element k , the gradient vector is computed and summed for each node i (from 1 to n) of the element. Taking into account that only gradient vectors of irregular nodes are summed, a coefficient α_i is introduced. The value of this coefficient is 1 when the determinant of the Jacobian is negative or null at the point i and 0 when $\det \mathbf{J}_i$ is positive. The procedure is then repeated for each distorted element. Finally, the residual vector is derived from the summation over p , where p is the index of all the elements in the mesh having the node j in their connectivity.

$$\mathbf{V}_j = \sum_p \sum_{i=1}^n \alpha_i \nabla(\det \mathbf{J}_i)_j \quad (2)$$

where $\alpha_i = 1$ if $\det \mathbf{J}_i \leq 0$ and $\alpha_i = 0$ if $\det \mathbf{J}_i > 0$.

The modification of node locations is based on equation (3) where X_j and X'_j are the old and the new coordinates of the node j , and w is a factor depending on the scale of the structure, taken here as a percentage of the average edge length, averLength , taking into account the dimension of the mesh. The directional vector is finally normalized with the Euclidian norm so that $\mathbf{V}_j / \|\mathbf{V}_j\|$ has no dimension.

$$X'_j = X_j + \frac{\mathbf{V}_j}{\|\mathbf{V}_j\|} * w * \text{averLength} \quad (3)$$

In addition to the algorithm, maximal node displacements are constrained so that the regularized mesh still fits the patient morphology. The constraints for internal and

external nodes differ but both of them are based on a percentage of the displacement of the nodes from their initial positions, computed after the mesh-matching algorithm (with a small percentage for external surface nodes in order to still fit the patient geometry). It is worth noting that the regularization method can be applied to any element type: tetrahedron, hexahedron, or wedge. It is also important to recognize that the limitation of the regularization method is its inability to guarantee that the algorithm will correct any irregular mesh. Indeed, due to its formulation, the iterative process of the algorithm tries to find a global solution, without any theoretical guarantee to converge.

3. Application to computer-aided orthognathic surgery

3.1 Orthognathic surgery

Orthognathic surgery (the “surgery to create straight jaws”, see Richter *et al.* (1998)) involves a wide variety of surgical procedures performed to reposition maxilla, mandible and the dento-alveolar segments to achieve facial and occlusal balance. This may be necessary due to congenital abnormalities, growth disturbances or trauma. Such corrections are largely achieved by osteotomies, surgical techniques by which parts of the jaw(s) are cut to create separate fragments, which can then be moved to new positions while preserving their blood supply. Correction of these abnormalities generally normalizes patients’ dental occlusion and temporo-mandibular joint function, and results in improvement in functions such as chewing, speaking and breathing, while often enhancing facial aesthetics.

3.2 Face modeling for the prediction of the surgical outcome

A model of the patient face used to simulate the morphological modifications following bone repositioning could greatly improve the planning of the intervention, for both the surgeon and the patient. Different models of the face soft tissue were proposed in the literature. A review can be found in Chabanas *et al.* (2003). Our methodology for the generation of patient-specific models was applied to the facial soft tissues. A generic FE model of the human face was therefore designed (figure 1a, see also Chabanas *et al.* (2003) for details). It is made of 2884 elements and 4216 nodes representing the soft tissues (skin, muscles and fat tissues) as a homogenous elastic material (small deformation hypothesis; Young modulus 15 kPa, Poisson’s ratio 0.49).

This generic model was used as a starting point to generate patients’ specific models. Seven patients’ models were automatically generated by our algorithm. For each model, the mesh-matching method was unable to create regular FE meshes (between 5 and 10% of the elements were detected as irregulars). The regularization algorithm

Table 1. Computational results for the regularization of the seven human face meshes.

Patient No.	Number of irregular elements	Number of iterations	Computation time (min)	Min. node disp. (mm)	Max. node disp (mm)	Mean node disp. (mm)	Number of shifted nodes
1	149	130	1	10^{-3}	2.69	0.22	614
2	291	350	1	6.2×10^{-5}	2.36	0.16	982
3	268	300	1	2.3×10^{-5}	3.36	0.21	1177
4	191	450	3	1.53×10^{-4}	4.40	0.31	773
5	234	350	4	7.8×10^{-5}	2.90	0.32	875
6	253	350	3	8.4×10^{-5}	2.49	0.30	840
7	239	350	3	2.05×10^{-4}	2.73	0.30	882

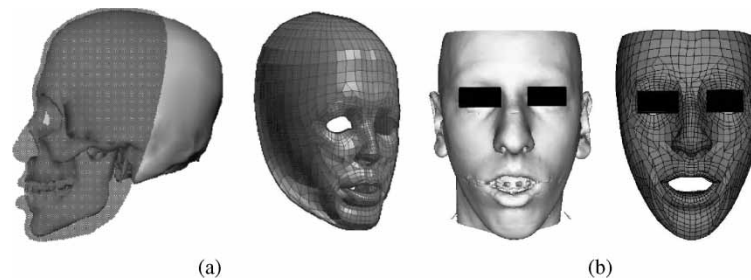


Figure 1. (a) Generic finite element model of the human face (from Chabanas et al. (2003)). (b) Preoperative patient CT scan (left) and FE model of the patient (right).

described above was, therefore, used to correct irregularities from the meshes. Table 1 summarizes, for each patient model, the regularization computation time with the corresponding number of iterations, the number of irregular nodes, node displacements and the number of shifted nodes. Depending of the patient model, it took 1–4 min (130–450 iterations) on a DEC Alpha 500 MHz computer to successfully correct all the irregular elements. For each patient, the new mesh remains very close to the one generated by the mesh-matching algorithm and no geometrical difference can be visually observed.

Figure 1b plots the regularized FE mesh generated for one of the patients. For this patient, osteotomies were simulated using a set of cutting planes interactively positioned on the 3D skeleton geometrical model reconstructed from the patient's CT scan (figure 2).

The deformations of the soft tissues are then simulated using the patient FE model. The bones' displacements define the boundary conditions for the model: inner nodes in contact with the non-modified skeleton surface are fixed, while the displacements are applied to the nodes on the osteotomized bone segments. Nodes around the osteotomy line are not constrained, to account for the bone-tissue separation due to the surgical access.

The rest of the nodes in the outer part of the mesh or in the mouth and cheek areas are left free to move. Once the outcome of the surgery has been simulated, it can be qualitatively compared with the post-operative skin surface of the patient, reconstructed from the CT scan. Figure 3 shows such a qualitative comparison.

For a given simulation of bone osteotomies, images are printed with different angles of view: frontal, left and right profile, left and right oblique views, and upper and lower views. An interactive 3D visualization is also available to magnify some areas or to use specific view angles. The deformed model and the patient reconstruction are observed next to each other, then in superposition. Emphasis is given to the perception of the model quality in the most relevant morphological areas in the face: cheek bones, lip area, chin and mandible angles.

4. Application to orbital surgery

4.1 Exophthalmia

Exophthalmia is an orbital pathology that affects the ocular muscles and/or the orbital fat tissues (Saraux *et al.* 1987). It is characterized by a forward displacement of the eye ball

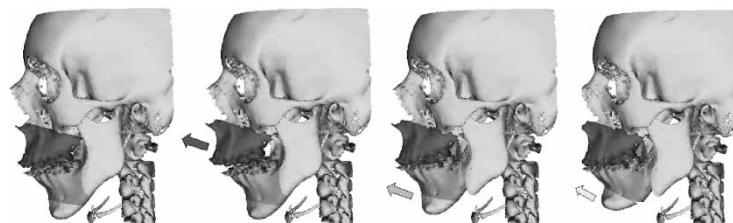


Figure 2. Simulation of maxilla, mandible and genial osteotomies. The osteotomies are simulated using a set of planes cutting the 3D reconstruction of the patient facial skeleton.

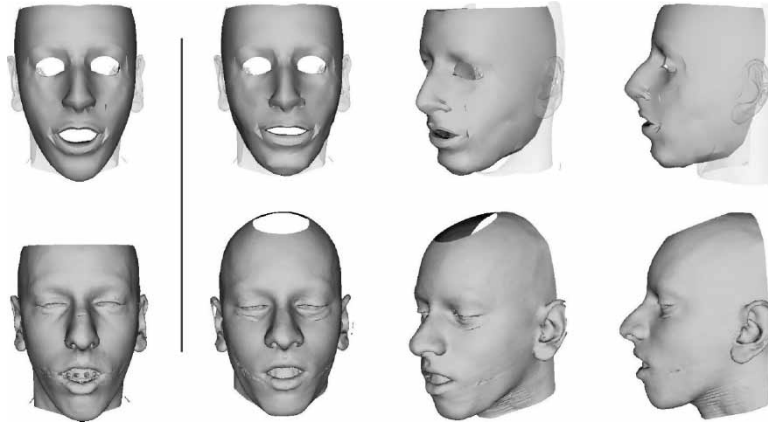


Figure 3. Qualitative evaluation. The simulations (top) are visually compared with the 3D reconstruction of the post-operative patient skin surface (bottom). Emphasis is given to the perception of the model quality in the most relevant morphological areas in the face: cheeks bones, lips area, chin and mandible angles.

outside the orbit. This displacement, called protrusion, may lead to aesthetic problems and to physiological disorders such as a tension of the optic nerve (dangerous for the patient vision) and the ocular muscles and/or an abnormal cornea exposition to the light. One of the treatments for exophthalmia is surgery—in particular, the technique of decompression of the orbit (Wilson and Manke 1991), defined by an osteotomy of a part of the orbital bone walls via an eyelid incision. This leads to an increase of the orbital volume, which thus offers more space to the soft tissues, particularly into the sinuses. To improve the backward displacement of the eye ball, some surgeons push on it in order to evacuate more of the fat tissues in the sinuses. Up to now, the prediction of the results of an exophthalmia reduction was based on clinical observations (Adenis and Robert 1994) that gave the following average law: for a 1 cm^3 soft tissues decompression, a backward displacement from 1–1.5 mm is expected. Even if this *a-posteriori* empiric result is interesting from a clinical point of view, it cannot be directly used for the surgery planning since it does not take into account the size of the osteotomy realized by the surgical gesture. To our knowledge, Luboz *et al.* (2004) were the first to propose a biomechanical model to assist in the planning of the exophthalmia reduction. This model is composed of 1375 elements and 6948 nodes that represent the soft tissues of the orbit, i.e. the

fat tissues, the muscles and the optic nerve as a homogeneous poroelastic material (figure 4). In this preliminary work, Luboz *et al.* have proposed a validation of their model in a clinical test.

4.2 FE models of the orbital soft tissues to predict consequences of decompression

Starting from the model proposed by Luboz *et al.* (2004)—the generic model of the orbital soft tissues—the algorithm described in section 2 was used to generate 11 new FE models from 11 patient CT data. Figure 4 plots two new patients FE model generated with our method. Table 2 summarizes, for each patient model, the regularization computation time with the corresponding number of iterations, the number of irregular nodes, node displacements and the number of shifted nodes.

Here again, as for the generation of FE human face model, our method succeeded in correcting all the irregular elements while preserving a mesh that is geometrically very close to each patient's morphology.

Then, each patient model was used to simulate a decompression gesture, followed by a pressure exerted onto the eyeball. The FE mechanical parameters (Young modulus, Poisson's ratio, porosity and permeability) were identically defined for all models, as the rheological variability among

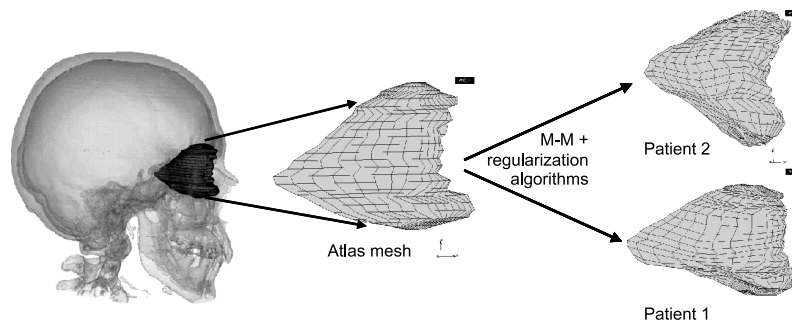


Figure 4. Application of the mesh-matching algorithm and the regularization phase to two patients with significant differences in orbit morphologies. The mesh at the center is the generic one (see Luboz *et al.* (2004), the eyeball is not plotted), that is deformed to fit the morphology of the other patients, thus creating patient-specific FE meshes.

Table 2. Computational results for the regularization of the eleven orbit meshes.

Patient No.	Number of irregular elements	Number of iterations	Computation time	Min. node disp. (mm)	Max. node disp (mm)	Mean node disp. (mm)	Number of shifted nodes
1	276	400	5 min	4.56×10^{-4}	2.451	0.338	927
2	202	200	3 min	1.81×10^{-4}	1.033	0.112	732
3	203	100	1 min	1.26×10^{-4}	1.21	0.115	798
4	211	600	7 min	1.07×10^{-4}	1.175	0.101	660
5	166	400	5 min	2.88×10^{-4}	1.135	0.103	728
6	9	30	30 s	0.03×10^{-4}	0.41	0.004	39
7	188	100	1 min	2.85×10^{-4}	1.03	0.094	697
8	11	30	30 s	0.05×10^{-4}	0.53	0.007	48
9	232	200	3 min	4.14×10^{-4}	0.959	0.121	787
10	237	300	4 min	1.56×10^{-4}	1.02	0.156	777
11	8	30	30 s	0.03×10^{-4}	0.39	0.004	37

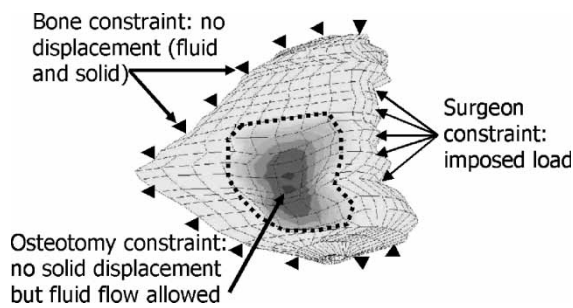


Figure 5. Boundary conditions applied to the orbital mesh to simulate the decompression surgery.

patients is unfortunately unknown. For each model, boundary conditions were set as the following (figure 5):

- (1) The constraint of the bone walls surrounding the soft tissues is translated by a nil displacement and a total sealing effect at the surface nodes.
- (2) Since the periost (the membrane around the soft tissues) remains after the wall osteotomy, it is still constraining the fat tissue elastic phase, while the fluid phase is able to flow through this opening. Consequently, the osteotomy surface nodes are fixed in displacement while they are

released in term of sealing effects.

- (3) To simulate the force exerted on the eyeball by the surgeon, an imposed axial load has been applied to all the nodes located at the soft tissue/eyeball interface.

Four different osteotomies sizes were simulated (0.8, 1.7, 3.4 and 5.9 cm²) for each of the 11 patients, leading to 44 simulations. From those results, we tried to study the relationship that could be extrapolated between the size of the osteotomy (the surgical gesture) and the backward displacement of the eyeball (the suited outcome of the surgery). Figure 6 plots, for each patient model, the laws that can be derived from these simulations.

As a first observation, these graphs clearly show the nonlinear influence of the surface on the backward eyeball displacement. A consequent increase of the osteotomy surface is needed to get a moderate increase of the backward displacement. Moreover, it can be noticed that the geometry of the orbit seems to have an influence on the relationship between the size of the osteotomy and the eyeball's backward displacement since a difference of about 50% can be measured between the two extreme patients. Despite those differences, an average law has been computed to estimate the relationship between the

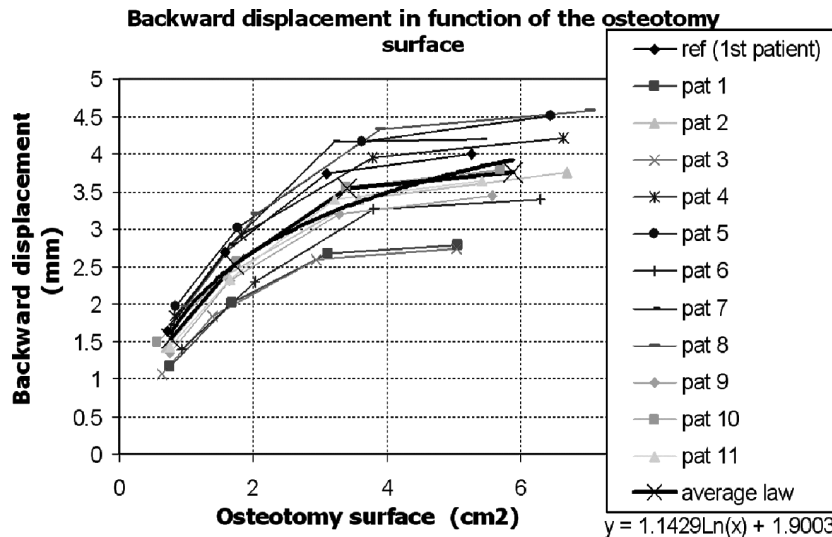


Figure 6. Influence of the osteotomy surface on the eyeball backward displacement for the 11 patients and average curve.

osteotomy surface and the eyeball backward displacement (figure 6, black curve). The corresponding equation gives the backward displacement $disp$ as a function of the osteotomy surface $surf$:

$$disp = 1.1 * \ln(surf) + 1.9 \quad (4)$$

From our point of view, this equation seems to be more useful to a surgeon than the 1 cm^3 versus $1/1.5 \text{ mm}$ relation proposed by Adenis and Robert (1994). Indeed, it gives an estimation of the osteotomy surface to perform, named $surf$, in order to obtain a certain eyeball backward displacement, $disp$.

5. Conclusion

This paper has introduced our methodology for the automatic generation of patient-specific FE models of anatomical structures. This methodology is based on two algorithms, namely the mesh-matching method, originally proposed by our group, followed by an original regularization technique based on the Jacobian matrix transform related to the FE reference element and the current element.

The patient-specific generation method was applied to two computer-assisted clinical interventions, namely the maxillofacial (orthognathic) and orbital (exophthalmia) surgeries. Seven patient-specific FE models of the facial soft tissues were therefore successfully generated. One of these models was used to predict the consequences of mandibular and maxillary bone displacements on the patient post-operative aesthetics. A qualitative comparison was provided between these predictions and the effective patient appearance, measured on a post-operative CT exam. Concerning exophthalmia, 11 FE models of orbital soft tissues were generated and used to extract, from simulations, an average law between the osteotomy surface (the surgical gesture) and the eyeball backward displacement (the outcome of the surgical gesture).

In the next phase, we plan to apply our methodology for the generation of patient-specific FE models to other clinical applications involving other geometrical FE models such as shoulder (Briot *et al.* 2004), upper airways (Chouly *et al.* 2003) and liver (Voinin *et al.* 2002). Another important innovation would be to include quality criteria for the FE mesh into the iterative regularization algorithm, like warping factor, parallel deviation, aspect ratio, edge angle, skew angle or twist angle.

Acknowledgements

Stéphane Lavallée is acknowledged for his contribution on the elastic registration algorithm used in this work. Franck Boutault (Maxillofacial Department, Toulouse Hospital, France) is acknowledged for providing the patient data and for discussions about the generation of patient-specific models.

References

- J.P. Adenis and P.Y. Robert, "Décompression orbitaire selon la technique d'Olivari", *J. Fr. Ophthalmol.*, 17(1), pp. 686–691, 1994.
- F.S. Azar, D.N. Metaxas and M.D. Schnall, "Methods for modeling and predicting mechanical deformations of the breast under external perturbations", *Med. Image Anal.*, 6, pp. 1–27, 2002.
- J.M. Blackall, A.P. King, G.P. Penney, A. Adam and D.J. Hawkes, "A statistical model of respiratory motion and deformation of the liver", *Lect. Notes Comput. Sci.*, 2208, pp. 1338–1340, 2001.
- J. Briot, D. Charvin, P. Mansat, M. Mansat and P. Swider, "Kinematics study in total shoulder arthroplasty using FEA", *Proceedings of the 6th International Symposium on Computer Methods in Biomechanics & Biomedical Engineering*, Madrid, 2004.
- M. Chabanas and Y. Payan, "A 3D finite element model of the face for simulation in plastic and maxillo-facial surgery", *Proceedings of the Third International Conference on Medical Image Computing and Computer-Assisted Interventions–MICCAI'2000*, Springer Verlag LNCS, 1935, pp. 1068–1075, 2000.
- M. Chabanas, V. Luboz and Y. Payan, "Patient specific finite element model of the face soft tissue for computer-assisted maxillofacial surgery", *Med. Image Anal.*, 7(2), pp. 131–151, 2003.
- F. Chouly, A. Van Hirtum, X. Pelorsson and Y. Payan, "Obstructive sleep apnea syndrome. Part 2: computer simulation of the fluid–structure interaction", *Arch. Physiol. Biochem.*, 111, p. 54, 2003.
- B. Couteau, Y. Payan and S. Lavallée, "The mesh matching algorithm: an automatic 3D mesh generator for finite element structures", *J. Biomech.*, 33(8), pp. 1005–1009, 2000.
- S. Lavallée, "Registration for computer-integrated surgery: methodology, state of the art", in *Computer Integrated Surgery*, R. Taylor, S. Lavallée, G. Burdea and R. Mosges, Eds., Cambridge, MA: MIT Press, pp. 77–97, 1996.
- S. Lavallée, P. Sautot, J. Troccaz, P. Cinquin and P. Merloz, "Computer assisted spine surgery: a technique for accurate transpedicular screw fixation using CT data and a 3D optical localizer", *J. Image Guided Surg.*, 1(1), pp. 65–73, 1995.
- V. Luboz, B. Couteau and Y. Payan, "3D finite element meshing of entire femora by using the mesh matching algorithm", *Transactions Editor in Proceedings of the Transactions of the 47th Annual Meeting of the Orthopaedic Research Society*, B.S. Trippel, Ed., Chicago, Illinois, USA., p. 522, 2001.
- V. Luboz, A. Pedrono, D. Ambard, F. Boutault, Y. Payan and P. Swider, "Prediction of tissue decompression in orbital surgery", *Clin. Biomech.*, 19(2), pp. 202–208, 2004.
- P. Merloz, B. Tonetti, A. Eid, C. Faure, S. Lavallée, J. Troccaz, P. Sautot, A. Hamadeh and P. Cinquin, "Computer assisted spine surgery", *Clin. Orthop.*, 337, pp. 86–96, 1997.
- G. Picinbono, H. Delingette and N. Ayache, "Non-linear anisotropic elasticity for real-time surgery simulation", *Graph. Models*, 65, pp. 305–321, 2003.
- M. Richter, P. Goudot, F. Laurent, A. Jaquinet and L. Bidaut, "Chirurgie correctrice des malformations ou dysmorphies maxillomandibulaires: bases chirurgicales", *Encyclopédie médico-chirurgicale, Stomatologie*, Paris: 22-066-E-10, 24 pages Elsevier, 1998.
- H. Sarau, B. Biais and C. Rossazza, *Ophthalmologie, Chap. 22: Pathologie de l'orbite*, Masson, Ed., 1987, pp. 341–353.
- O. Skrinjar, A. Nabavi and J. Duncan, "Model-driven brain shift compensation", *Med. Image Anal.*, 6, pp. 361–373, 2002.
- R. Szeliski and S. Lavallée, "Matching 3-D anatomical surfaces with non-rigid deformations using octree-splines", *Int. J. Comput. Vision*, 18(2), pp. 171–186, 1996.
- S.L. Taylor, G. Burdea, and R. Mosges (Eds.), *Computer Integrated Surgery*, Cambridge, MA: MIT Press, pp. 77–97, 1996.
- G. Touzot and G. Daht, "Une représentation de la méthode des éléments finis. Collection université de Compiègne", 1984.
- D. Voinin, Y. Payan, M. Amavizca, C. Létoublon and J. Troccaz, "Computer-aided hepatic tumour ablation: requirements and preliminary results", *C.R. Biologies*, 325, pp. 309–319, 2002.
- W.B. Wilson and W.F. Manke, "Orbital decompression in Graves' disease. The predictability of reduction of proptosis", *Arch. Ophthalmol.*, 109, pp. 343–345, 1991.
- O.C. Zienkiewicz and R.L. Taylor, *The Finite Element Method*, 4th ed., McGraw-Hill Book Company, 1994.